ADVANCED MATERIALS INTERFACES
Open Access
www.advmatinterfaces.de

Adsorber Charge Dominates over Hydrophobic or Fluorophilic Functionalization in Influencing Adsorption of PFCA onto Polystyrene Resins

Florian Junge, Philipp Wittwer, Thomas Sommerfeld, Lennart Gehrenkemper, Christian Zoister, Philip Nickl, Matthias Koch, Björn Meermann, and Rainer Haag**

A systematic series of industrial-relevant polystyrene-based anion exchange resins that are functionalized with hydro- or fluorocarbon chains are compared regarding their adsorption behavior toward perfluorocarboxylic acids (PFCA) in respect to their charge, chain length, and type of chain. The results clearly show the dominance of electrostatic interactions in the adsorption process as uncharged adsorber materials showed no adsorption at all. In contrast, the charged adsorber materials showed in general a PFCA removal of 80% to 30% over the experiment depending on effluent fraction. Unexpectedly, for perfluorobutanoic acid (PFBA) the highest removal rate is found with consistently >90%. Despite observing significant benefits in the adsorption of PFCA for fluoroalkylated adsorbers in comparison to their non-fluorinated counterparts, this effect of fluoroalkylation is comparatively small and can not be clearly attributed to fluorophilic interactions between the fluoroalkyl chains. These findings help clarifying that the introduction of fluorocarbon moieties in adsorber materials is not necessary in order to remove fluorocarbon molecules from the environment.

1. Introduction

In recent years, the environmental and health hazards of per- and polyfluorinated alkyl substances (PFAS) have gained enormous scientific and public attention. Their plentiful exceptional properties led to their wide range of industrial and private uses, for example, in water-resistant coatings, as foaming agents in fire extinguishers, or in textiles.[1,2] This excessive use of these highly persistent organic pollutants without proper recycling techniques led to a global contamination of water reserves, soil, air, and living organisms. A plethora of adverse health effects are associated with the intake of PFAS including kidney and liver toxicity, decreasing immune response to vaccinations, and carcinogenicity.[3–5] The United States Environmental Protection Agency therefore released interim updated lifetime drinking water health advisories for the concentration of certain PFAS in municipal water as little as 4 pg L^{-1} (for perfluorooctanoic acid; PFOA)[3] similar to other regulatory environmental authorities worldwide.[4,6]

Efficient large-scale removal of persistent and bio-accumulative PFAS to meet future legal requirements remains a challenging field of analytical chemistry and material synthesis. Techniques that were investigated for PFAS removal include adsorption, electrochemical capture, reverse osmosis, and nanofiltration.[7–9] For example, Baldaguez et al.[10] developed polymers with redox-active metallocene sidechains which can bind negatively charged PFAS when connected to the cathode while releasing them again after connecting the polymer to the anode. It was discovered that an increase in electron affinity and a decrease in redox potential leads to higher PFAS capture and release. Also, it was found that a combination of amine and fluoroalkyl groups on the redox-active polymer synergistically facilitates the electrochemical capture of short-chain PFAS.[11] For the development of high-capacity and selective adsorber materials for PFAS it is crucial to gain as much understanding of influential factors on PFAS adsorption as possible. It is widely assumed that Van-der-Waals interactions (in form of the hydrophobic effect), and electrostatic interactions are the main driving forces for the adsorption of PFAS onto industrial-relevant adsorber materials especially activated carbon and polymeric resins.[1,12–14] However, the hydrophobic effect as well as electrostatic interactions are not PFAS-specific and are also known for binding other types of inorganic ions or organics.[12] For example, the presence of 2.3 ppm glucose and 3.2 ppm bovine serum

F. Junge, C. Zoister, P. Nickl, R. Haag
Institut für Chemie und Biochemie
Freie Universität Berlin
Takustr. 3, 14195 Berlin, Germany
E-mail: haag@chemie.fu-berlin.de
P. Wittwer, T. Sommerfeld, L. Gehrenkemper, M. Koch, B. Meermann
Federal Institute for Materials Research and Testing, BAM
Richard-Willstätter-Straße 11, 12489 Berlin, Germany
E-mail: bjoern.meermann@bam.de
The ORCID identification number(s) for the author(s) of this article can be found under https://doi.org/10.1002/admi.202400199

DOI: 10.1002/admi.202400199

albumin decreased the adsorption isotherm of perfluorooctyl sulfonic acid (PFOS) on activated carbon by 87%[15] and the presence of 2.03 mmol L^{-1} chromate ions decreased the PFOS adsorption capacity of Amberlite IRA67 by roughly 40% and significant chromate adsorption was observed.[16] To increase the selectivity for PFAS removal, a handful of publications investigated the suitability of fluoroalkylated materials, ranging from covalent organic frameworks[17,18] over metal-organic frameworks,[19–21] inorganic minerals,[22–25] polymers,[26–29] molecular-imprinted polymers,[30–32] and gels[33–38] to polymeric fibers,[39] as adsorber for PFAS. The hypothesis in common states that fluoroalkylated adsorbers exhibit either attractive interactions towards fluoroalkylated analytes or repelling interactions to non-fluoroalkylated analytes resulting in an overall favor of fluoroalkylated analytes. In multiple fields including biphasic catalysis, microfluidics, and supramolecular assembly of surfactants there is evidence of these attractive fluorophilic interactions which occur exclusively between PFAS molecules.[40,41] The results of the before-mentioned studies that use fluoroalkylated adsorbers for PFAS adsorption generally confirm this hypothesis and thus further support the concept of beneficial fluorophilic interactions between fluoroalkylated adsorbers and analytes. Du and co-worker,[22] for example, observed a better adsorption of PFOS onto vermiculite that was spiked with 3-(((perfluorooctyl)sulfonyl)amino)-*N,N,N*-trimethyl propylammonium iodide (which contributed a fluoroalkyl group as well as a cationic group to the adsorber) and magnetite nanoparticles. There are also works that avoid charged adsorbers at all and prove PFAS adsorption on neutral fluoroalkylated hydrogels.[33]

The upfield shift of the CF_3 signal at ≈−80 ppm in the ^{19}F-NMR spectrum by up to 2 ppm is considered as proof for fluorophilic interactions between the adsorber and the fluorinated analyte in many of these works.[24,28,29,33,36] However, the quantitative impact of fluorophilic interactions during PFAS adsorption remains unclear, that is, the tested adsorbers were not compared to their non-fluorinated counterparts with functional alkyl chains of equal length with two exceptions: Choudhary and Bedrov[38] compared the adsorption of GenX-PFAS onto a set of four polystyrene- or poly(tetrafluorostyrene)-based cationic gels with (*N,N,N*-trimethylammonium)-ethoxy cationic sites which were cross-linked with polyethylene glycol (PEG) or perfluoropolyethyer (PFPE) in molecular dynamics simulations. While the fluorinated polystyrene backbone was superior to the non-fluorinated polystyrene backbone for PFAS adsorption, the presence of the perfluoroalkyl groups of the PFPE did not led to a relevantly increased adsorption of PFAS in comparison to the PEG cross-linked gels, apparently due to the long distance of fluoroalkyl groups and cationic charge. Kumarasamy et al.[34] observed adsorption of PFAS onto their hydrogels only when it was functionalized with both fluoroalkyl groups (specifically PFPE) and quaternary ammonium ions indicating synergistic effects between charged and fluorinated sides. Their hydrogels bearing only tertiary amines or PEG instead of PFPE only marginally adsorbed PFAS. Besides the studies of Song et al.[24] and Zhang et al.,[17] we are further not aware of any study examining the influence of the type of fluoroalkyl group on the adsorption capacity or selectivity to certain PFAS. Song and co-workers functionalized glass slides with fluoroalkylated silanes ($Cl_3SiC_6H_4F_9$, $Cl_3SiC_8H_4F_{13}$, and $Cl_3SiC_{10}H_4F_{17}$) to adsorb volatile PFAS from the gas phase. No clear trend of the adsorption of PFAS depending on the chain length of the functionalization was observed. Zhang and co-workers equipped a porous aromatic framework (PAF) with either CF_3- or C_2F_5-groups. The PAF with CF_3 groups showed slightly faster kinetics and lower residual PFAS concentration than the PAF with C_2F_5 which in turn showed a higher maximum adsorption capacity.

Negatively charged PFAS, namely perfluorocarboxylic acids (PFCA) and perfluorosulfonic acids (PFSA), are among the most commonly analyzed PFAS in the environment. One of our key motivations was to study the effect of the length of the perfluoroalkyl group of the PFAS on its adsorption in dependence on the functional group of the adsorber material. To facilitate this aim, we decided to focus our investigation solely on PFAS with one common head group. Consequently, we decided to measure and compare the PFCA removal efficiency of anion exchange resins that were functionalized with either linear fluorocarbons or hydrocarbon chains of varying lengths. We used these data to conclude which type of hydrophobic group (chain length and fluorocarbon/hydrocarbon) results in the most promising functionalized resins for the adsorption of PFCA. Because the observed difference between the different functionalizations was rather small, we further compared the adsorption to a set of uncharged polystyrene resins equipped with the same functional groups. As no adsorption was observed for the uncharged resins under the same conditions, these findings corroborated the dominance of the adsorbers charge over the type of hydrophobic group during the adsorption process.

2. Results and Discussion

2.1. Choice and Preparation of Adsorbers

Since the focus of our work is the determination of the impact of the type of hydrophobic group of the adsorber material on its adsorption of PFCA, comparison of the adsorption behavior of a systematic series of adsorber materials with several different functionalizations is required. Polystyrene (PS) resins were therefore chosen as ideal starting material for further functionalization due to a high surface area, large-scale availability, and industrial relevance.[12,42] PFCA are anionic species so the PS resins of choice were anion exchange resins. Only two types of PS-based anion exchange resins are used in large-scale industrial applications. On the one hand, weak anion exchange resins possess primary (aminomethyl-) or tertiary amine groups ((*N,N*-dialkylamino)methyl-PS) and, thus, are sensitive to pH but usually allow relatively easy desorption and adsorber regeneration during washing cycles. On the other hand, strong anion exchange resins possess quaternary ammonium groups ((*N,N,N*-trialkylammonium)methyl-PS) which results in a more robust adsorption but usually more challenging desorption.[42–44] The amine groups in weak anion exchange resins are good nucleophiles. We expected that they could be functionalized with electrophilic fluoroalkylation agents leading to fluoroalkylated anion exchange resins that are similar in structure to commercial resins for PFAS adsorption (e.g., AmberLite PSR2 Plus,[45] Lewatit TP 108 DW,[46] Purofine PFA694[47]).

We selected two (*N,N*-dimethylamino)methyl-PS functionalized weak anion exchange resins,[48,49] Purolite A100Plus and

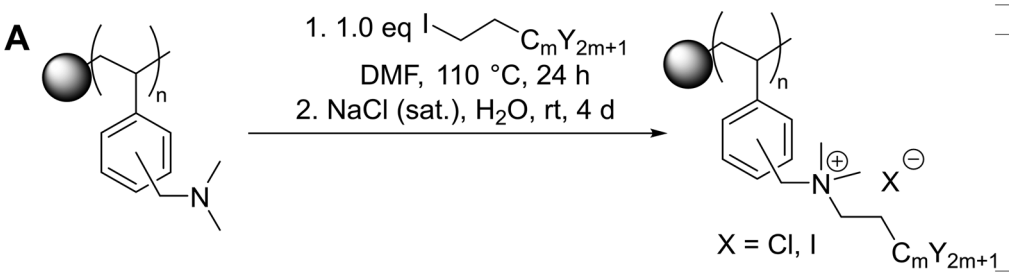

Adsorber	m	Y
LW-C4	2	H
LW-C6	4	H
LW-C8	6	H
LW-C10	8	H
LW-C4F5	2	F
LW-C6F9	4	F
LW-C8F13	6	F
LW-C10F17	8	F

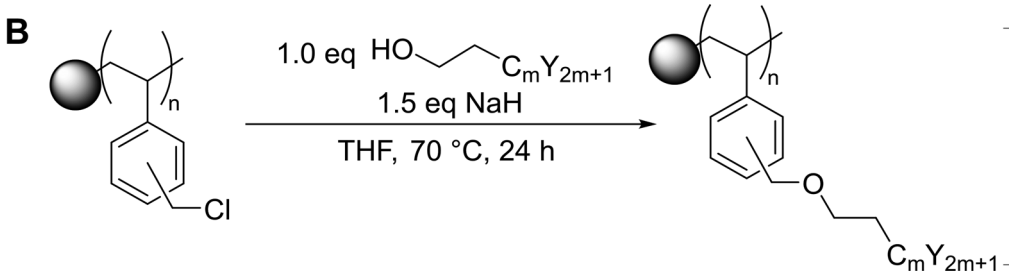

Adsorber	m	Y
MF-C4	2	H
MF-C6	4	H
MF-C8	6	H
MF-C10	8	H
MF-C4F5	2	F
MF-C6F9	4	F
MF-C8F13	6	F
MF-C10F17	8	F

Figure 1. Functionalization reactions of the charged A) and of the uncharged B) adsorbers. The shaded circles symbolize the resin beads.

Lewatit MP 62 WS for functionalization with linear fluoroalkyl iodides of the type $I(CH_2)_2(CF_2)_nCF_3$. The spacer of two methylene groups between the iodide and the perfluorocarbon chain is the minimum to favor the heterolytic cleavage of the carbon iodine bond over its homolytic cleavage. Nevertheless, fluoroalkyl iodides with two methylene groups as spacers can be deprotonated by a wide range of bases (alkoxides, hydroxides, etc.) due to the strong inductive effect of the perfluoroalkyl group resulting in elimination instead of substitution. Fluoroalkyl iodides with longer spacers would circumvent potential eliminations[50] but would lead to overall less fluorinated products with greater distance between the fluorophilic chain and electrostatic charge and are considerably harder to obtain. Fluoroalkylation or respective alkylation of the adsorber was performed in a simple one-step reaction by heating the resin (without the addition of base to prevent elimination) in a solution of the respective (fluoro)alkyl iodide in dimethyl formamide (DMF). The work up was intentionally kept as simple as possible by only including filtration and drying steps in order to reduce the possibility for discrepancy between the resins. Despite their very similar structure, the Purolite A100Plus resin degraded during (fluoro)alkylation so we continued our study with (fluoro)alkylated Lewatit MP 62 WS as the charged resins.

A series of (fluoro)alkylated uncharged polystyrene resins was prepared as a control to study the effect of the charge. Here we kept the sequence of the respective chain identical except for the charge and only replaced the ammonium with an ether group. The corresponding (fluoro)alkylated ethers in the adsorber side chain were obtained by a one-step Williamson ether synthesis from a chloromethylated polystyrene resin with comparable concentration of functional groups, divinyl benzene-induced crosslinks and mesh size.[51] The length of functional side chains from the heteroatom for both resins, charged (LW-) and uncharged (MF-), were 4, 6, 8, and 10 carbon atoms which equal a fluorocarbon chain length of 2, 4, 6, and 8 fluorinated carbon atoms, respectively (**Figure 1**).

2.2. Adsorber Characterization

The elemental composition of all adsorbers was first determined using elemental analysis (Tables S4 and S5, Supporting Information). For the charged adsorbers, we were not able to get reproducible values. In general, each drying step increased the C/H/N content.

Therefore we chose to analyze the elemental composition of all charged adsorbers before the adsorption of PFCA via XPS (Figure S2; Table S3, Supporting Information). In order to determine the conversion rate of amine groups for the charged fluoroalkylated adsorbers the ratio of fluorine to nitrogen content as determined by XP survey spectra quantification was divided by the amount of fluorine atoms per side chain. This value can then be used to estimate the amount of fluoroalkyl groups per gram of adsorber (**Table 1**, for details see SI). Additionally, we calculated the ammonium ion densities of the adsorbers based the sum of the chlorine and the iodine content as no complete ion exchange to chlorine could be achieved. All materials show similarly high ratios of halide to nitrogen (≥81%), showing that most nitrogen atoms are present as charged ammonium groups. The so-calculated amount of ammonium ions (2.82–3.48 mmol g^{-1}) is higher than the amount of fluoroalkyl groups (0.36–0.48 mmol g^{-1}). We propose that this discrepancy is caused by the occurrence of Hofmann elimination. After the successful substitution reaction at the fluoroalkyl group the β-H, which is strongly acidified by the presence of the fluorine atoms, can undergo this elimination. This produces an alkene and a protonated ammonium group with an unchanged counter ion. The presence of the alkene is supported by the IR spectra which show a small adsorption band at 3020 cm^{-1}, which is commonly assigned to alkenes[52] (see **Figure 2**A for LW-C6F9 as an example, see Supporting Information for all IR spectra) and also not found in the starting material. Additionally, the ^{19}F-NMR shows two peaks around -80 ppm (Figure 2C) which indicates the presence of two CF_3-Groups with different magnetic environments.

Table 1. Analysis of adsorber resins after functionalization with (fluoro)alkyl groups before the adsorption of PFCA by their F/N ratio, halide content, and iodide content obtained from quantified XP survey spectra.

Resin	(Cl + I)/N [%]	R_4N^+ ion density [mmol g^{-1}]	I/N [%]	Minimum amount (fluoro)alkyl chains after synthesis [mmol g^{-1}]	F_x/N[a)] [%]	Fluoro alkyl chains [mmol g^{-1}]
LW-C4	95 ± 12	3.4 ± 0.1	62 ± 4	2.24 ± 0.04		
LW-C6	84 ± 11	3.2 ± 0.1	54 ± 4	2.06 ± 0.05		
LW-C8	101 ± 15	3.3 ± 0.1	67 ± 7	2.16 ± 0.05		
LW-C10	87 ± 13	2.9 ± 0.1	61 ± 5	2.00 ± 0.05		
LW-C4F5	90 ± 8	3.48 ± 0.09	42 ± 3	1.63 ± 0.04	12 ± 1	0.48 ± 0.03
LW-C6F9	107 ± 12	3.2 ± 0.1	48 ± 5	1.47 ± 0.04	14 ± 1	0.44 ± 0.02
LW-C8F13	99 ± 3	3.3 ± 0.1	44 ± 3	1.47 ± 0.03	10.9 ± 0.8	0.36 ± 0.01
LW-C10F17	81 ± 7	2.82 ± 0.09	37 ± 2	1.30 ± 0.03	10.4 ± 0.7	0.364 ± 0.009

[a)] F_x equals the fluorine content in at% divided by x, where x represents the number of fluorine atoms in the side chain; e.g., x = 5 for LW-C4F5.

Lastly, the amount of iodide ions indicate that more fluoroalkyl groups were present in the material directly after the synthesis, since iodine can only occur as ion after a successful substitution reaction.

Therefore we assume the fluorine content as found by XPS does not represent the functionalization degree after synthesis. As conclusion of the previous statement, the iodine content in the material gives the minimum degree of amine conversion after the synthesis. Since the chloride ions could be introduced by either ion exchange with a iodide or a hydroxide ion (formed by protonation of free amine group with water), it is not possible to make reliable assumptions above the minimum degrees as indicated by the iodine content. The minimum degrees of functionalization after the reaction is 37% – 48% (1.30–1.63 mmol g^{-1}) for the fluoroalkylated adsorbers (Table 1).

For the non-fluorinated charged adsorbers we could not estimate the amount of alkyl side chains at the time point of the XPS measurements due to the lack of a reference element like fluorine. However, we can again use the iodine content as the minimum degree of functionalization (54% – 67%, 2.00–2.24 mmol g^{-1}). The fluorinated and unfluorinated charged adsorber materials show a similar range for the degrees of minimum functionalization, but all unfluorinated adsorber materials show higher minimum functionalization degrees.

For the uncharged resins we did not find indications for elimination. Therefore we used the elemental analysis as the basis for the following calculations. As expected from their molecular formulas, all alkylated uncharged resins showed an increase in the carbon content upon functionalization while all fluoroalkylated uncharged resins showed a drop in the carbon content. The amount of (fluoro)alkyl chains were calculated using the observed change in the carbon content. This showed that the uncharged adsorbers contained less (fluoro)alkyl groups than the charged ones (Table S2, Supporting Information).

Due to the considerable error of both techniques, elemental analysis, and XPS, for the determination of the degree of functionalization of the adsorbers, we decided to apply a unified (fluoro)alkylation procedure instead. This means that we only determine the overall capability of the respective type of functionalized resin (chain length, charge, and fluorination) for PFCA adsorption in a qualitative manner including all of the following, ease of incorporation, side chain stability, and PFCA removal efficiency.

Infrared spectroscopy revealed the characteristic C—F stretching vibration from 1200 to 1050 cm^{-1} for most fluoroalkylated adsorbers (Figure 2A,B; Figures S11 and S13, Supporting Information) as a further qualitative proof of functionalization.[41] The spectra of MF-C6F9, MF-C8F13, and MF-C10F17, however, only showed a small signal in that regime (Figure S13, Supporting Information). This might be attributed to the seemingly overall lower degree of functionalization of uncharged adsorbers in comparison to the charged adsorbers (Table 1). Additionally, in the spectra of the charged adsorbers the C—N stretching vibration at 1255 cm^{-1} and the C—H stretching vibrations (for CH_2 and CH_3 groups in α-position to amines) at 2812 and 2761 cm^{-1} vanish upon functionalization as it is expected during the transition from tertiary amine to quaternary ammonium.[52] Scanning electron microscopic images of both types of adsorbers, charged and uncharged, reveal no visual change during functionalization (Figures S14–S31, Supporting Information) and higher porosities of the uncharged resins. The macroscopic structure of the resins, thus, seemed to stay intact. Nevertheless, the charged resins were highly brittle, and the formation of nanometer-sized debris was observed after applying any amount of mechanical force (e.g., during attempted washing procedures).

Solid-state NMR spectra were recorded for LW-C6, LW-C6F9, and the unfunctionalised Lewatit resin (Figure S3, Supporting Information). The ^{13}C total suppression of sidebands (TOSS) spectrum of LW-C6F9 showed a fluorocarbon signal at 107 ppm, while LW-C6 shows intense hydrocarbon signals between 7 ppm and 33 ppm. At ≈60 ppm the signal of methylene groups attached to the ammonium can be detected. The ^{19}F-NMR spectrum of LW-C6F9 confirmed the presence of fluoroalkyl groups (Figure 2C).

2.3. PFOA Removal Efficiency

To elaborate the effect of the type of hydrophobic group used for functionalization of the resin on the adsorption of PFCA, the resins were compared by their efficiency of adsorbing PFOA, one of the most prominent PFAS, in a small column set up (Figure S1, Supporting Information). A total volume of 200 mL of an aqueous PFOA solution was passed over a column (400 mg

adsorber/≈1 mL bed volume) and the eluate was collected in fractions of 25 mL. Quantification of the remaining PFOA concentration in the effluent was performed by liquid chromatography-tandem mass spectrometry (LC-MS/MS).

At the beginning, we needed to find a suitable concentration that allowed us to detect a change in adsorption on the charged adsorber LW-C6F9 within the 200 mL of PFOA solution. We started at 0.05 mg L^{-1}, but to our surprise, very high concentrations of 500 mg L^{-1} PFOA were required for an observable drop of adsorption for the chosen experimental condition of 200 mL of eluent. The saturation curve of most charged adsorbers at these conditions (**Figure 3A**) were similar, except LW-C10 adsorbing consistently worst while LW-C6F9 adsorbed the best. As the degree of functionalization could not be determined exactly, the results should be considered as qualitative comparison. In three reference runs through the column set up (without any adsorber added as negative control) and in separate runs with both of the unfunctionalized resins (LW-Ref and MF-Ref) no decrease in PFOA concentration was detected except in the last fraction of LW-Ref (Figure 3). This surprising, reproducible late-term decrease of PFOA concentration for LW-Ref might indicate some sort of surface reaction rather than a classic adsorption which would be expected already in earlier fractions. Nevertheless, the overall PFOA removal efficiency of LW-Ref under our tested conditions is small in comparison to the functionalized charged resins. Despite fluoroalkylated adsorbers generally showing slightly higher PFOA adsorption then non-fluoroalkylated ones of the same chain length, we decided to repeat the adsorption of PFOA on LW-C6F9 since it showed the highest difference when compared to the alkylated LW-C6. In the repetition, LW-C6F9 showed an adsorption behavior similar to the other charged adsorbers (**Figure 4**). In contrast to the charged adsorbers, none of the uncharged adsorbers was adsorbing any detectable amount of PFOA at this high concentration (Figure 3B). Even if the generally lower amount of (fluoro)alkyl groups in the uncharged adsorbers (Table 1; Figure S1, Supporting Information) are considered, these results show the dominance of electrostatic interactions for PFOA adsorption while (fluoro)alkylation of the uncharged polystyrene adsorber seems to be insufficient for PFAS adsorption.

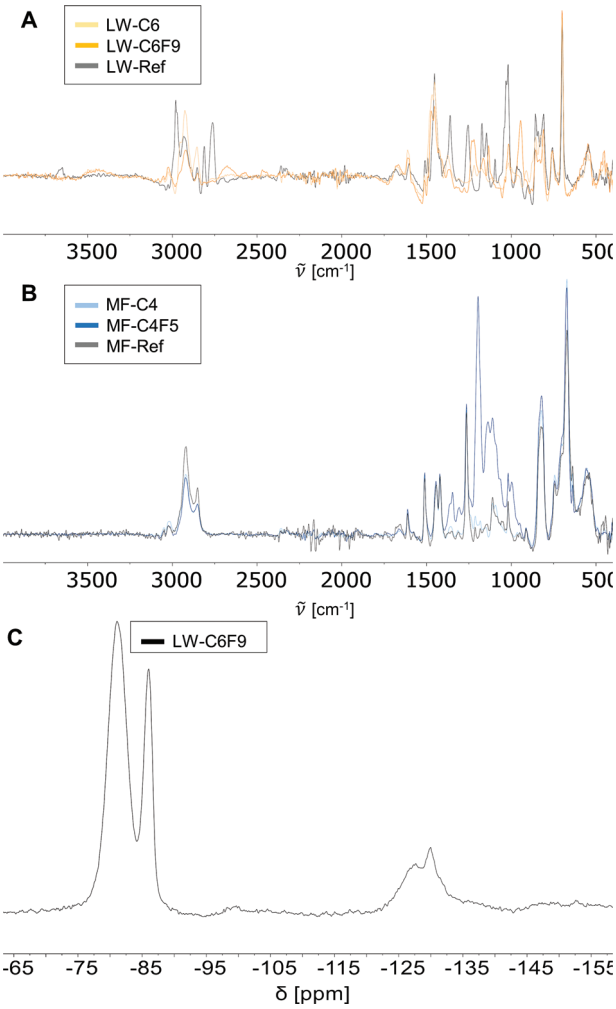

Figure 2. A) FTIR spectra of LW-C6, LW-C6F9, and LW-Ref, B) FTIR spectra of MF-C4, MF-C4F5, and MF-Ref. C) Solid state TOSS ^{19}F-NMR spectra of LW-C6F9.

2.4. Adsorption of other PFCA

Fluorophilic interactions are known to be stronger with increasing length of the fluorocarbon chain.[53] If attractive fluorophilic interactions between the fluoroalkyl chains are the reason behind the previously observed enhanced adsorption of PFOA onto fluoroalkylated charged adsorbers then the difference in the PFCA adsorption between fluoroalkylated and alkylated adsorbers would increase with increasing chain length of the PFCA. The adsorption of a series of PFCA, perfluorobutyric acid (PFBA), perfluorohexanoic acid (PFHxA) and perfluorononanoic acid (PFNA) was therefore compared to the adsorption of an equimolar solution of PFOA onto LW-C6 and LW-C6F9 (Figure 4). We decided to use equimolar solutions in order to keep a constant ratio of PFCA molecules to available adsorption sites.

Unexpectedly, shorter PFCA consistently adsorbed better on both adsorbers than longer PFCA. This observation is contrary to most previously published adsorption data of PFAS where usually longer PFAS bind better to the adsorber than their shorter derivatives, presumably due to an increased hydrophobicity.[1,12,44,54] The few publications that observed a similar trend for the adsorption of short-chain PFAS onto anion exchange resins attributed it to the faster kinetics of the short-chain PFAS molecules into the pores of the adsorber.[54–56] As our contact times of 0.3–3 min are short, too, the greater adsorption of short-chain PFCA onto LW-C6 and LW-C6F9 is likely a kinetic effect. This would explain why the long-chain PFCA is more readily adsorbed in the first fractions as the easiest reachable adsorption sites on the outer surface are then occupied. In addition to LC-MS/MS, we confirmed the successful adsorption of PFBA and PFOA on LW-C6 and LW-C6F9 via XP survey spectra where a sharp increase in fluorine content and decrease in iodine and chlorine content was detected (Table S8, Supporting Information).

A least squares-based linear regression (at a significance level of $\alpha = 0.05$) was used to evaluate the significance

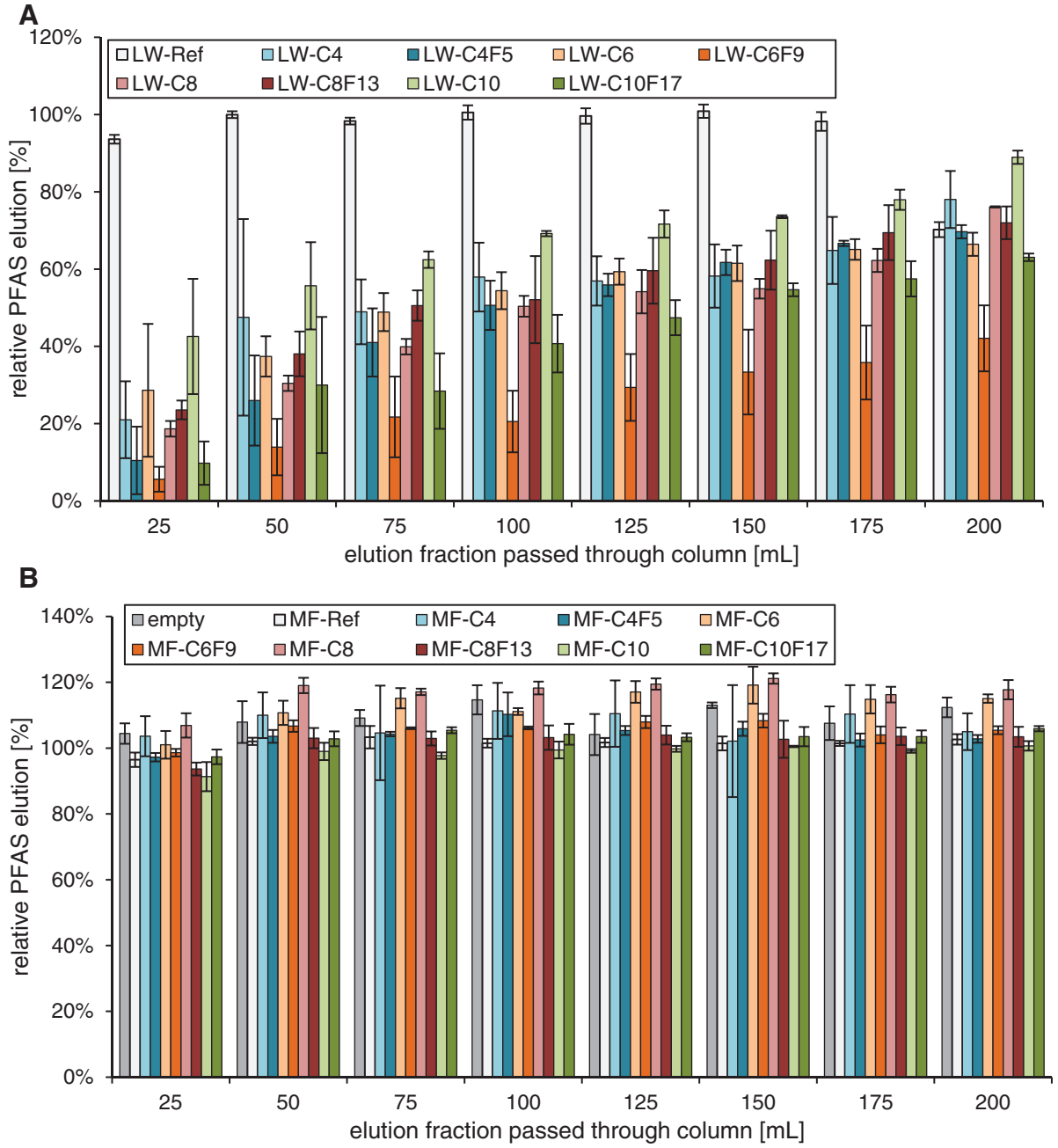

Figure 3. Ratios of the remaining PFOA concentration in the effluent after passing through a column with the respective adsorber and the original PFOA concentration (c_0 = 500 mg L^{-1} ≈ 1.2 mmol L^{-1}). A charged and B uncharged adsorbers including a reference without adsorber. All experiments were performed in independent triplicates. Error bars are the standard deviation (n = 3).

and contribution of the studied parameters (length of the adsorber side chain, length of the PFCA, the presence of a fluoroalkylated side chain in the adsorber, adsorber charge and eluent fraction) on the PFCA removal efficiency of the functionalized resins during the first 100 mL of PFCA solution (Figure S4A, Supporting Information). Noteworthy, the analyte solution was passed over the columns solely by gravity which led to empty bed contact times of 0.3 to 3 min which changed frequently even within a fraction and were hard to control. As its reliable measurement was not possible and no correlation to the type of adsorber was observed, it was not treated as a separate variable and ignored. Reliable quantification of the factors that contribute to the PFCA adsorption was impossible in the regression because of the uncertainties in the exact adsorber composition. Anyhow, the regression confirmed qualitatively the observed dominating impact of the charge of the adsorber compared to all other variables. Due to the huge discrepancy of the adsorption performance of charged and uncharged adsorbers and the overwhelming impact of the charge, the inclusion of the uncharged adsorbers led to a possible bias, heteroscedasticity (Figure S5, Supporting Information), and

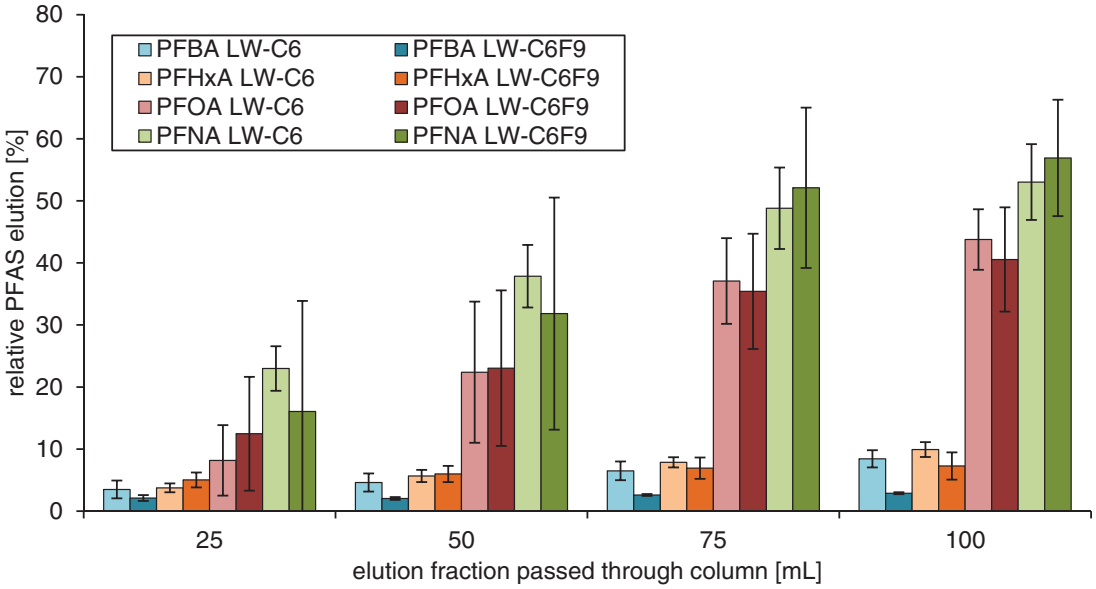

Figure 4. Ratios of the remaining concentration of PFBA, PFHxA, PFOA, and PFNA after passing through a column filled with LW-C6 or LW-C6F9 to the original concentration (c_0 = 1.2 mmol L^{-1}). All experiments were performed in independent duplicates. The error bars are the standard deviation (n = 2).

significant lack-of-fit of the model without any valuable input to the model (besides for the evaluation of the impact of the charge). To address these aspects, a second more accurate but still qualitative regression without the data of the uncharged adsorbers was performed (Figure S4B, Supporting Information) for the evaluation of all non-charged related variables between each other. Significant trends included an increased PFCA adsorption of fluoroalkylated adsorbers in comparison to the non-fluoroalkylated adsorbers which was independent from all other variables. Further, reducing the length of the hydrophobic chain (in general) will lead to an increased removal of PFOA with an optimum at a chain length of 6. Optimization of either of these two variables (chain length or fluoroalkylation) leads to a similar change in expected PFOA removal (Equations S25 and S26, Supporting Information).

3. Conclusion

The qualitative comparison of the saturation curves for the adsorption of PFOA onto fluoroalkylated and alkylated, charged, and uncharged polystyrene-based adsorbers corroborated the dominance of electrostatic interactions during adsorption of PFCA. Furthermore the saturation curves for the adsorption of PFOA, PFBA, PFHxA, and PFNA showed that PFBA and PFHxA were remarkably well adsorbed by LW-C6 and LW-C6F9. Both the fluoroalkylation and chain length of the adsorber contribute to a similar degree to the adsorption of PFCA.

The slightly superior adsorption of PFCA on fluoroalkylated over alkylated adsorbers was independent of the length of the fluoroalkyl group and of the length of the PFCA in the eluent. If preferential fluorophilic interactions contribute significantly to the adsorption, an increased adsorption of long-chained PFCA onto fluoroalkylated adsorbers in relation to non-fluoroalkylated adsorbers would be expected. Moreover, one would expect a higher increase of PFCA removal of the fluoroalkylated adsorbers versus their non-fluoroalkylated counterparts the longer the (fluoro)alkyl chain is. The major impact of charge over fluorophilic interaction that we found in our adsorption studies indicate that neither the enhanced adsorption of PFCA onto fluoroalkylated adsorbers can be clearly attributed to fluorophilic interactions (as proposed by many authors)[17,24,28,34] nor does it seem to be dominated by hydrophobic effects (as proposed by Xie et al.).[26] Similar results to ours were found by Erkal et al.[21] who concluded that the generally superior adsorption of PFAS onto fluoroalkylated adsorbers are likely not caused by a direct attractive fluorophilic interaction between the fluoroalkyl chains. Further, Huang et al.[37] also identified electrostatic interactions as dominant interaction for the adsorption of PFAS onto fluoroalkylated charged adsorber materials. Even if fluorophilic interaction would drive the adsorption of PFAS onto adsorbers, non fluoroalkylated adsorbers will also have these after a first layer of PFAS molecules is bound to the adsorber material. The reasoning being that then the surface of the adsorbers now also possess a fluoroalkylated shell. This thought would be in line with the concept of the adsorbers of Du et al.[22,23] and Erkal et al.[21] who purposely adsorbed PFAS onto non-fluoroalkylated adsorber materials to increase their PFAS adsorption performance.

Future research should consider the investigation of other hydrophobic groups for adsorber functionalization other than fluoroalkyl groups, such as branched alkyl chains or hydrocarbon chains with carbonyl groups that exhibit electron withdrawing effects on the site of the charge (similar to fluoroalkyl groups) to further evaluate what causes the general higher adsorption of PFAS onto fluoroalkylated materials. Furthermore, it is important to extend future studies from PFCA to other regulated PFAS classes like PFSA, perfluoroalkylated sulfonamides or telomeric alcohols. According to our results the influence of the fluorophilic interaction on the PFCA removal does not compensate for their

negative environmental impact.[5,57] As a practical conclusion from this study, developers of PFAS adsorbers should focus on good electrostatic properties of their materials rather than the use of fluorinated alkyl chains.

4. Experimental Section

Materials: Sodium hydride (60 w% dispersion in mineral oil), the chloromethylated polystyrene resin (product number: 63 868), hexan-1-ol (98%), octan-1-ol (99%), PFOA (96%), PFNA (97%), PFHxA (97%), 3,3,4,4,5,5,6,6,7,7,8,8,8-Tridecafluoro-1-iodooctane (96%) and decan-1-ol (98%) were purchased from Sigma-Aldrich (Taufkirchen, Germany). Butan-1-ol (99%) was purchased from Grüssing (Filsum, Germany). Lewatit MP 62 WS was a gift from Lanxess (Cologne, Germany) and was washed with THF under reflux and dried before use. 3,3,4,4,4-Pentafluorobutan-1-ol (97%) was purchased from Fluorochem (Hadfield, UK). 1H,1H,2H,2H-Nonafluorohexan-1-ol (97%), 1-iodobutane (98%), 1-iodohexane (97%), and 1-iodooctane (97%) were purchased from TCI (Eschborn, Germany). 1H,1H,2H,2H-Perfluorooctan-1-ol (97%), 3,3,4,4,4-pentafluoro-1-iodobutane (97%), 1-iododecane (98%), 3,3,4,4,5,5,6,6,7,7,8,8,8-Tridecafluoro-1-iodooctane (97%), 1H,1H,2H,2H-perfluoro-1-iododecane (97%) and 1H,1H,2H,2H-perfluorodecan-1-ol (97%) were purchased from abcr (Karlsruhe, Germany). PFBA (99%) was a product from Alfa Aesar (Haverhill, USA). Sodium chloride (99.5%) was purchased from Fisher (Schwerte, Germany). 3,3,4,4,5,5,6,6,6-Nonafluoro-1-iodohexane (95%) was purchased from Biosynth (Bratislava, Slovakia).

Fourier Transform Infrared Spectroscopy: Fourier transform infrared spectra were recorded on an Alpha II FT/IR spectrometer (Bruker Optik GmbH) with platinum attenuated total (ATR) unit (monolithic diamond crystal) and Bruker's OPUS software. 24 scans were recorded with a resolution of 4 cm^{-1}. Spectra were displayed using MestReNova version 14.1.1-24571 (Mestrelab Research S.L.). Whittaker smoothening was applied to correct the baselines of the spectra. The resins were grinded to powder prior to the measurement.

X-Ray Photon Spectroscopy: NAP-XPS experiments were performed with an EnviroESCA spectrometer (SPECS Surface Nano Analysis GmbH, Berlin, Germany), equipped with a monochromatic Al Kα X-ray source (Excitation Energy = 1486.71 eV) and a PHOIBOS 150 electron energy. Samples for XPS analysis were prepared on indium foil. The spectra were measured in normal emission, and a source-to-sample angle 60° was used. All spectra were acquired in fixed analyzer transmission (FAT) mode. The binding energy scale of the instrument was calibrated, following a technical procedure provided by SPECS Surface Nano Analysis GmbH (calibration was performed according to ISO 15 472). For quantification, the survey spectra were acquired at ultra-high vacuum conditions with a pass energy of 100 eV, and the spectra were quantified utilizing the empirical sensitivity factors that were provided by SPECS Surface Nano Analysis GmbH (the sensitivity factors were corrected with the transmission function of the spectrometer). For charge compensation, the highly-resolved XP spectra were acquired under near-ambient pressure conditions (5 mbar H_2O) with a pass energy of 50 eV, and the respective data were fitted using UNIFIT 2020 data processing software. For fitting, a Shirley background and a Gaussian/Lorentzian sum function [peak shape model GL (30)] were used. If not denoted otherwise, the L-G mixing component was set to 0.30 for all carbon peaks and 0.40 for all heteroatom peaks. All binding energies were calibrated to the signal observed for the aliphatic C—C bond component (E_{bind} = 285 eV) if not stated otherwise.

Solid-State Nuclear Magnetic Resonance: Solid-state nuclear magnetic resonance spectra were recorded on a JEOL 600 ECZ R at a temperature of 2.4–23.3 °C. The ^{13}C-NMR frequency was 150.91 MHz, while the ^{19}F-NMR frequency was 564.73 MHz. Magic angle spinning was done with a frequency of 10 kHz (for LW-Ref 9 kHz were used instead). The contact time was 2 ms. The spectra were recorded under a total suppression of side bands (TOSS) with a relaxation time of 5 s. Spectra were displayed using MestReNova version 14.1.1-24571 (Mestrelab Research S.L.). The spectra were phase-corrected, and apodized (exponential: 100 Hz) and the base line was corrected using manually picked points if necessary. The resins were grinded to powder prior to the measurement.

CHN Elemental Analysis: Elemental analysis was carried out on a VARIO EL III instrument (Elementar, Hanau, Germany) using sulfanilic acid as the standard. The resins were grinded to powder prior to the measurement.

Adsorption of PFCA: The respective PFCA was dissolved in MilliQ water (c = 1.2 mmol L^{-1}) 1 d before the experiment with the assistance of an ultrasonic bath. All PFCA-containing solutions were handled at any time during the experiment in polypropylene or polyethylene vessels and contact to glass was excluded. (400 ± 2) mg of the respective ion exchange resins were filled into a column with polyethylene frit at the bottom, a pad from polypropylene fleece on top (to prevent the lighter adsorbers from floating) and washed with MilliQ water (10 mL). As the charge of the adsorber was introduced through the functionalization reaction, the resins were not further preconditioned with acid as recommended by the producer. The wetted columns from ion exchange resin had a volume of 1.0 to 1.1 mL. Twenty or forty times 5.00 mL aliquots of the respective PFCA solution were passed over the column. The eluate was collected in fractions with 25 mL each. The flow rate was between 0.3 and 3 mL min^{-1} resulting in empty bed contact times of 0.3 to 3 min.

Liquid Chromatography-Tandem Mass Spectrometry (LC-MS/MS) Analysis of PFCA Solutions: Aliquotes of the collected fractions were diluted with MilliQ by a factor of 2500 in two steps (first to a factor of 25 and then to a factor of 100) and then mixed in a 1/1 (v/v)-ratio with HPLC grade methanol (except for LW-Ref and MF-Ref) in a fluorine-free polypropylene LC vial. Chromatographic separation was achieved using an Agilent ZORBAX RRHD Eclipse Plus C18, 3 mm × 100 mm, 1.8 µm column installed on an Agilent 1290 Infinity II UHPLC system consisting of the following modules: Agilent 1290 Infinity II High-Speed Pump (G7120A), Agilent 1290 Infinity II Multisampler with Multiwash Option (G7167B) and Agilent 1290 Infinity II Multicolumn Thermostat (G7116B).

A gradient elution was performed with 5 mM ammonium acetate in water (mobile phase A) and methanol (mobile phase B) at 0.4 mL min^{-1} with a total run time of 17 min (Table S6, Supporting Information). To minimize background PFAS contamination, the Agilent PFC-Free HPLC Conversion Kit (part number 5004 0006) and a PFC delay column (part number 5062 8100) for delaying potential per- or polyfluorochemicals impurities from the mobile phases was installed on the UHPLC system.

Dynamic MRM (dMRM) analysis was performed using a 6495C LC/TQ with an Agilent Jet Stream (AJS) ion source operated in negative ionization mode. Data acquisition and processing were performed using Agilent MassHunter Data LC/MS Acquisition software version 10.0 and Quantitative Analysis software version 10.2, respectively. PFAC30PAR (Wellington Laboratories) was used as an analytical mix standard containing 30 PFAS compounds in methanol. Further instrument conditions can be found in Table S7 (Supporting Information). The measured concentrations of the respective PFCA were divided by the measured concentration of the native PFCA solution (without contact to the column) to determine the relative PFCA elution. Two relative PFCA elution values (one of the LW-Ref elution fraction 125 mL and one of MF-C8F13, elution fraction 100 mL) were above 140%, far outside the possible elution regime as well as not reproducible in the replicates, that they were excluded from all data representation and analysis. Further, one of the effluent solutions of LW-C8, fraction 200 mL, was excluded because it showed a relative PFOA concentration of 2.4% while its replicates showed a PFOA concentration of (76.1 ± 0.2)%.

Synthesis of Uncharged Adsorber Materials: A schlenk flask with the chloromethylated polystyrene resin (1.0 eq. of Cl) was repeatedly flame dried under vacuum. Dry tetrahydrofuran (THF) (10 mL per 1 g resin) was added. The reaction mixture was cooled with an ice bath and sodium hydride (1.5 eq.) stabilized in mineral oil was added portion wise. Upon completion of hydride addition the respective (fluoro)alcohol (1.0 eq.) was slowly dropped to the dispersion. The mixture was refluxed for 24 h at 70 °C (when extensive foaming occurred the foam was washed back into the reaction flask with dry THF) and afterward quenched with water (10 mL) in an ice bath. If the mixture became too viscous during quenching, toluene was added for dilution. The resin was filtered off and washed with water

(250 mL) and THF (250 mL). Subsequently, the resins were stirred in THF (250 mL) for at least one night, filtered off, and washed with THF. The fluorinated resins were additionally refluxed in THF (250 mL) twice for 9–14 h respectively until the eluted THF became transparent. The functionalized resins were obtained as slightly yellow spheres after drying for 1 day at 60–80 °C.

Synthesis of Charged Adsorber Materials: Previously washed and dried Lewatit MP 62 WS (DVB-crosslinked (dimethylamino)methyl polystyrene) (13.0 g, 1.0 eq. of amine groups), dry DMF (40 mL) and the respective (fluoro)alkyl iodide (1.0 eq.) were added to a flame dried flask. The mixture was stirred for 24 h at 110 °C. The resins were filtered off and washed with THF (≈80 mL). Subsequently, the fluoroalkylated resins were refluxed in THF (400 mL) for 17 h while the non-fluorinated resins were stirred in THF (400 mL) at room temperature for 1 day. The resins were filtered off, washed with THF, and dispersed in a saturated aqueous sodium chloride solution (500 mL). The resins were filtered off after four days and washed with distilled water (300 mL). The functionalized resins were obtained as yellow spheres after drying for 6 day at 100 °C.

Statistical Data Analysis: The uncertainties of the functionalization degrees of the charged adsorbers were calculated using Gaussian uncertainty propagation either with the aid of the formulas presented in the Supporting Information or with the aid of the National Institute of Standards and Technology (NIST) Uncertainty Machine.[58,59]

The adsorption data of the functionalized resins was statistically analyzed using JMP Pro 16.0.0 (SAS Institute Inc.).[60] The relative PFCA elution in % set as a response variable. Relative PFCA elution of >100% were expected to be impossible in practice and the respective were set to 99.99% for statistical purposes as the response variable was defined in the range of [0; 1]. Fluorination and charge of the adsorber were used as categorical variables (yes/no), the chain length of PFCA and of the adsorber side chain and the fraction were used as discrete numeric variables. Despite not being in the focus of the study, the fraction was included as a variable in the analysis as it increased the amount of data points in comparison to the case where each fraction would be analyzed separately. Because the data is not available for all the adsorption tests and the temporal evolution of adsorption not the main interest only the first 4 fractions were taken into the analysis to still be able to analyze all relevant interactions. With the given set of data it was impossible to modulate the effect of the degree of adsorber functionalization as this would require multiple adsorbers with the same functionalization but varying degrees of functionalizations. Linear regression (least square method with logit transformation of the response) gave the most accurate description of the adsorption of PFCA. It was applied to the complete data set (only the first 4 fractions, ANOVA F-test: $p < 0.0001$, lack of fit F-test: $p < 0.0001$, $R^2 = 0.9361$, $R^2_{adjusted} = 0.9329$) and in a second reduced model (ANOVA F-test: $p < 0.0001$, lack of fit F-test: $p = 0.2229$, $R^2 = 0.8116$, $R^2_{adjusted} = 0.8003$) applied to data that was obtained from charged adsorbers only. All main effects and first-order interaction effects as well as quadratic and cubic effects (for numeric variables) were included in the model if below the significance limit of $\alpha = 0.05$ or component of an significant interaction effect. The quadratic effect of the fraction was removed from the model of the complete data despite being significant as it led to an increase in adsorption in the fourth fraction which did not seem to align with the raw data. In the reduced model, anyhow, it was included and aligned well with the raw data. The studentized residual of three data points of uncharged adsorbers were outside the 95% confidence interval even after considering Bonferroni correction and thus excluded as regression outliers.

Supporting Information

Supporting Information is available from the Wiley Online Library or from the author.

Acknowledgements

The authors would like to thank Andrea Schulz for the gold sputtering of the samples for SEM analysis, the core unit BioSupramol (especially Dr. Andreas Schäfer, Gregor Drendel, Fabian Klautzsch, and Eleonore Christmann) for performing elemental analysis, Fourier transform infrared spectroscopy and solid-state nuclear magnetic resonance spectroscopy. Also, the authors would like to thank Dr. Olaf Wagner and Dr. Alejandro Sanchez for fruitful discussions and suggestions throughout the project and Dr. Yannic Kerkhoff for the discussion about the statistical analysis. All acknowledged authors are affiliated with the Freie Universität Berlin. The authors would like to thank Dr. Dirk Steinhilber (Lanxess Deutschland GmbH) and Purolite GmbH for providing Lewatit MP 62 WS and Purolite A100Plus free of charge. Gefördert durch die Deutsche Forschungsgemeinschaft (DFG) – Projektnumber (387284271 – SFB 1349). Funded by the Deutsche Forschungsgemeinschaft (DFG, German Research Foundation) – Project-ID (387284271 – SFB 1349).

Open access funding enabled and organized by Projekt DEAL.

Conflict of Interest

Both weak anionic exchange resins, Lewatit MP 62 WS and Purolite A100Plus, were provided free of charge from the respective manufacturers to perform this study. There are no financial interests of the authors associated with the study.

Author Contributions

The project was conceptualized by R.H., B.M., F.J., P.W., and L.G. The adsorbers were functionalized and characterized by F.J. and C.Z., PFCA adsorption was performed by F.J. and P.W. and PFCA quantification via LC-MS by T.S. and M.K. P.N. performed and analyzed XPS measurements. F.J. analyzed the data statistically. All authors contributed to the text of the manuscript and supporting information.

Data Availability Statement

The data that support the findings of this study are available in the supplementary material of this article.

Keywords

fluorophilic interactions, ion exchange resins, PFAS adsorption, water treatment

Received: March 2, 2024
Revised: May 21, 2024
Published online: June 4, 2024

[1] R. Amen, A. Ibrahim, W. Shafqat, E. B. Hassan, *Sustainability* **2023**, *15*, 16173.
[2] F. Suja, B. K. Pramanik, S. M. Zain, *Water Sci. Technol.* **2009**, *60*, 1533.
[3] Environmental Protection Agency, [FRL 9855–01–OW], Federal Register 2022, 87, No. 118, https://www.govinfo.gov/content/pkg/FR-2022-06-21/pdf/2022-13158.pdf (accessed: January 2024).
[4] B. Umwelt, N. S. Verbraucherschutz, *Guidelines for PFAS assessment*, www.bmuv.de/fileadmin/Daten_BMU/Download_PDF/Bodenschutz/pfas_leitfaden_2022_en_bf.pdf (accessed: January 2024).
[5] A. B. Lindstrom, M. J. Strynar, E. L. Libelo, *Environ. Sci. Technol.* **2011**, *45*, 7954.
[6] *Australian Government Department of Health, Health Based Guidance Values for PFAS*, https://www.health.gov.au/sites/default/files/documents/2022/07/health-based-guidance-values-for-pfas-for-use-in-site-investigations-in-australia_0.pdf (accessed: January 2024).

[7] A. Román Santiago, P. Baldaguez Medina, X. Su, *Electrochim. Acta* **2022**, *403*, 139635.
[8] C. T. Vu, T. Wu, *Crit. Rev. Env. Sci. Tec.* **2022**, *52*, 90.
[9] S. Yadav, I. Ibrar, R. A. Al-Juboori, L. Singh, N. Ganbat, T. Kazwini, E. Karbassiyazdi, A. K. Samal, S. Subbiah, A. Altaee, *Chem. Eng. Res. Des.* **2022**, *182*, 667.
[10] P. Baldaguez Medina, V. Ardila Contreras, F. Hartmann, D. Schmitt, A. Klimek, J. Elbert, M. Gallei, X. Su, *ACS Appl. Mater. Interfaces* **2023**, *15*, 22112.
[11] A. R. Santiago, S. Yin, J. Elbert, J. Lee, D. Shukla, X. Su, *J. Am. Chem. Soc.* **2023**, *145*, 9508.
[12] T. H. Boyer, Y. Fang, A. Ellis, R. Dietz, Y. J. Choi, C. E. Schaefer, C. P. Higgins, T. J. Strathmann, *Water Res.* **2021**, *200*, 117244.
[13] I. Ross, J. McDonough, J. Miles, P. Storch, P. Thelakkat Kochunarayanan, E. Kalve, J. Hurst, S. S. Dasgupta, J. Burdick, *Remediat. J.* **2018**, *28*, 101.
[14] F. Dixit, R. Dutta, B. Barbeau, P. Berube, M. Mohseni, *Chemosphere* **2021**, *272*, 129777.
[15] S. Deng, Q. Yu, J. Huang, G. Yu, *Water Res.* **2010**, *44*, 5188.
[16] J. Yu, L. Lv, P. Lan, S. Zhang, B. Pan, W. Zhang, *J. Hazard. Mater.* **2012**, *225-226*, 99.
[17] C. Zhang, J. Dong, P. Zhang, L. Sun, L. Yang, W. Wang, X. Zou, Y. Chen, Q. Shang, D. Feng, G. Zhu, *Natl. Sci. Rev.* **2023**, *10*, nwad191.
[18] J. Huang, Y. Shi, G. Z. Huang, S. Huang, J. Zheng, J. Xu, F. Zhu, G. Ouyang, *Angew Chem. Int. Ed. Engl.* **2022**, *61*, e202206749.
[19] J. Xie, F. Sun, C. Wang, Q. Pan, *Materials (Basel)* **2016**, *9*, 327.
[20] H. Wang, L. Yu, Y. Lin, J. Peng, S. J. Teat, L. J. Williams, J. Li, *Inorg. Chem.* **2020**, *59*, 4167.
[21] T. S. Erkal, N. Shamsuddin, S. Kirmizialtin, A. O. Yazaydin, *J. Phys. Chem. C* **2023**, *127*, 3204.
[22] Z. Du, S. Deng, S. Zhang, W. Wang, B. Wang, J. Huang, Y. Wang, G. Yu, B. Xing, *Environ. Sci. Technol.* **2017**, *51*, 8027.
[23] Z. Du, S. Deng, S. Zhang, B. Wang, J. Huang, Y. Wang, G. Yu, B. Xing, *J. Phys. Chem. C* **2016**, *120*, 16782.
[24] Y. Song, Y. Wu, D. Wu, X. Ma, S. Jiang, Z. Peng, C. Zhang, Y. Yin, R. Guo, *Environ. Int.* **2023**, *180*, 108205.
[25] E. K. Stebel, K. A. Pike, H. Nguyen, H. A. Hartmann, M. J. Klonowski, M. G. Lawrence, R. M. Collins, C. E. Hefner, P. L. Edmiston, *Environ. Sci.: Water Res. Technol.* **2019**, *5*, 1854.
[26] R. Xie, L. Zhou, A. E. Smith, C. B. Almquist, J. A. Berberich, N. D. Danielson, *J. Hazard. Mater.* **2022**, *431*, 128521.
[27] H. Tang, Y. Gou, Z. Yan, Q. Hu, F. Zhang, Q. Xiao, Y. Zhong, W. Zhu, *Microporous Mesoporous Mater.* **2020**, *305*, 110398.
[28] X. Tan, M. Sawczyk, Y. Chang, Y. Wang, A. Usman, C. Fu, P. Král, H. Peng, C. Zhang, A. K. Whittaker, *Macromol.* **2022**, *55*, 1077.
[29] X. Tan, J. Zhong, C. Fu, H. Dang, Y. Han, P. Král, J. Guo, Z. Yuan, H. Peng, C. Zhang, A. K. Whittaker, *Macromol.* **2021**, *54*, 3447.
[30] H. Guo, Y. Liu, W. Ma, L. Yan, K. Li, S. Lin, *J. Hazard. Mater.* **2018**, *348*, 29.
[31] J. M. Steigerwald, S. Peng, J. R. Ray, *ACS ES&T Eng.* **2023**, *3*, 520.
[32] F. Cao, L. Wang, Y. Tian, F. Wu, C. Deng, Q. Guo, H. Sun, S. Lu, *J. Chromatogr. A* **2017**, *1516*, 42.
[33] Q. Quan, H. Wen, S. Han, Z. Wang, Z. Shao, M. Chen, *ACS Appl. Mater. Interfaces* **2020**, *12*, 24319.
[34] E. Kumarasamy, I. M. Manning, L. B. Collins, O. Coronell, F. A. Leibfarth, *ACS Cent. Sci.* **2020**, *6*, 487.
[35] Y. Koda, T. Terashima, M. Takenaka, M. Sawamoto, *ACS Macro Lett.* **2015**, *4*, 377.
[36] Y. Koda, T. Terashima, M. Sawamoto, *J. Am. Chem. Soc.* **2014**, *136*, 15742.
[37] P. J. Huang, M. Hwangbo, Z. Chen, Y. Liu, J. Kameoka, K. H. Chu, *ACS Omega* **2018**, *3*, 17447.
[38] A. Choudhary, D. Bedrov, *ACS Macro Lett.* **2022**, *11*, 1123.
[39] P.-Y. Chen, B. Wang, S. Zhuang, Y. Chen, Y.-P. Wei, *Colloids Surf., A* **2021**, *619*, 126539.
[40] F. Junge, P. W. Lee, A. Kumar Singh, J. Wasternack, M. P. Pachnicz, R. Haag, C. A. Schalley, *Angew Chem. Int. Ed.* **2023**, *62*, e202213866.
[41] R. J. Baker, P. E. Colavita, D. M. Murphy, J. A. Platts, J. D. Wallis, *J. Phys. Chem. A* **2012**, *116*, 1435.
[42] K. Dorfner, in *Ion Exchangers* (Ed: K. Dorfner), Walter de Gruyter, Berlin, New York, **1991**, pp. 33–34.
[43] M. Riegel, S. Egner, F. Sacher (Concawe), *Review of water treatment systems for PFAS removal*, https://www.concawe.eu/wp-content/uploads/Rpt_20-14.pdf (accessed: January 2024).
[44] C. T. Vu, T. Wu, *Environ. Sci.: Water Res. Technol.* **2020**, *6*, 2958.
[45] *DuPont, Product Data Sheet AmberLite™ PSR2 Plus Ion Exchange Resin, Form No. 45-D00899-en, Rev. 2*, https://www.dupont.com/content/dam/dupont/amer/us/en/water-solutions/public/documents/en/IER-AmberLite-PSR2-Plus-PDS-45-D00899-en.pdf (accessed: January 2024).
[46] Lanxess Deutschland G. H., *PRODUCT INFORMATION LEWATIT® TP 108 DW, Version 2021-10-22*, https://lanxess.com/api/products/filehandlertds?tdsId=62526194&language=en-GB&clientId=50010&productItemId=5FF8A98C0AF245AD9DE975890D1FF726 (accessed: January 2024).
[47] *Purolite, Product Data Sheet Purofine® PFA694*, https://www.purolite.com/product-pdf/PFA694.pdf (accessed: January 2024).
[48] G. H. Lanxess Deutschland, *PRODUKTINFORMATION LEWATIT® MP 62 WS, Version 2019-09-16*, https://lanxess.com/api/products/filehandlertds?tdsId=04355024&language=de-DE&clientId=50010&productItemId=0B71DD8EF978441289043284679E4368 (accessed: January 2024).
[49] *Purolite, PRODUCT DATA SHEET Purolite A100Plus*, https://www.purolite.com/product-pdf/A100PLUS.pdf (accessed: January 2024).
[50] N. O. Brace, L. W. Marshall, C. J. Pinson, G. Van Wingerden, *J. Org. Chem.* **2002**, *49*, 2361.
[51] M. KGaA, *(Chloromethyl)polystyrene*, https://www.sigmaaldrich.com/DE/en/product/aldrich/63868 (accessed: January 2024).
[52] E. Pretsch, P. Bühlmann, M. Badertscher, *Spektroskopische Daten zur Strukturaufklärung organischer Verbindungen*, Springer, Berlin, Heidelberg, **2010**, Vol. *5*, pp. 273–298.
[53] T. Hasegawa, *Chem. Rec.* **2017**, *17*, 903.
[54] W. Wang, X. Mi, Z. Zhou, S. Zhou, C. Li, X. Hu, D. Qi, S. Deng, *J. Colloid Interface Sci.* **2019**, *557*, 655.
[55] D. N. Kothawala, S. J. Kohler, A. Ostlund, K. Wiberg, L. Ahrens, *Water Res.* **2017**, *121*, 320.
[56] S. Englund, *Master Thesis*, Swedish University of Agricultural Sciences, Uppsala, **2015**.
[57] Z. Abunada, M. Y. D. Alazaiza, M. J. K. Bashir, *Water* **2020**, *12*, 3590.
[58] T. Lafarge, A. Possolo, *NCSLI Measure* **2016**, *10*, 20.
[59] A. Possolo, T. Lafarge (NIST), *Uncertainty Machine — User's Manual*, https://tsapps.nist.gov/publication/get_pdf.cfm?pub_id=913874 (accessed: February 2024).
[60] *JMP® Version 16.0.0 ed.*, SAS Institute Inc., Cary, NC **1989** – **2024**.